Reorientation of Rotating Fluid in Microgravity Environment With and Without Gravity Jitters

R. J. Hung,* C. C. Lee,† and K. L. Shyu‡
University of Alabama in Huntsville, Huntsville, Alabama 35899

In a spacecraft design, the requirements of a settled propellant are different for tank pressurization, engine restart, venting, or propellant transfer. The requirement to settle or to position liquid fuel over the outlet end of the spacecraft propellant tank prior to main engine restart poses a microgravity fluid behavior problem. In this paper, the dynamical behavior of liquid propellant, fluid reorientation, and propellant resettling have been estimated through the use of a super computer CRAY X-MP to simulate the fluid management in a microgravity environment. Results show that the resettlement of fluid can be accomplished more efficiently for fluids in a rotating tank than in a nonrotating tank. Also, better performance can be achieved for imposed oscillatory motions on the fluid tank because of less time needed to accomplish fluid resettlement, and less time between the initiation and termination of geysering.

Nomenclature

a = radius of the circular cylinder
f_0 = frequency of gravity jitters, defined by Eq. (13)
g = gravitational acceleration
g_b = background gravity environment, defined by Eq. (13)
g_0 = Earth gravitation, $=9.81$ m/s^2
L = length of the cylinder
n = unit vector normal to the interface
P = pressure
r = cylindrical coordinate along radial direction
t = time
u = velocity component along radial direction
v = velocity component along circumferential direction
w = velocity component along axial direction
z = cylindrical coordinate along axial direction
δ = Dirac delta function
ζ = viscous coefficient of the second kind
η = profile of interface between gaseous and liquid fluids, defined by Eq. (7)
θ = cylindrical coordinate along circumferential direction
μ = viscous coefficient of the first kind
ν = kinematic viscosity coefficient
ρ = density
σ = surface tension of the interface
τ_{ij} = viscous stress tensor
ϕ = tangent of interface, defined by Eq. (12)
ω = rotating angular velocity of cylinder

Subscripts

G = gaseous fluid
L = liquid fluid

Received Oct. 30, 1989; revision received Feb. 19, 1990.

*Professor. Associate Fellow AIAA.
†Staff Engineer.
‡Graduate Student.

I. Introduction

SURFACE tension plays an important role in a large variety of fluid flows. The equilibrium shape of the free surface for unsteady state rotating fluid is governed by the balance of capillary, bulk pressure, viscous, centrifugal, and gravity forces, whereas steady-state rotating fluids are characterized by a solid rotation that is independent of viscosity. The configuration of the interface between liquid and gaseous fluids will be modified greatly when the gravity field is reduced to microgravity levels. In a microgravity environment, the instability of a liquid surface can be induced by the presence of longitudinal and lateral accelerations, vehicle vibration, and rotational fields of spacecraft. Slosh waves are thus excited, which produce high- and low-frequency oscillations in the liquid propellant. The sources of the residual accelerations range from the effects of the Earth's gravity gradient, atmospheric drag on the spacecraft, and spacecraft attitude motions to the higher-frequency "g-jitter" arising from machinery vibrations, thruster firings, and crew motions. A recent study[1] suggests, however, that the high-frequency accelerations may be unimportant in comparison to the residual motions caused by low-frequency accelerations.

In spacecraft design, the requirements for a settled propellant are different for tank pressurization, engine restart, venting, or propellant transfer. Prepressurization requires that heat- and mass-transfer effects be minimized; otherwise, a process of chilldown of the tank, venting of non-condensing gases, etc., may have to be carried out for the cryogenic system. For engine restart, it is necessary to have the liquid settle with no bubbles near the tank outlet so that the initial flow of propellant will not carry vapor to the pump or engine. The slosh wave amplitude should be relatively low to keep the center of mass (C.M.) shifts within an acceptable range and wave motion low enough to avoid pressure collapse caused by interface agitation. For venting, it is probably necessary that virtually all bubbles be displaced from the bulk liquid so that a two-phase mixture is not vented. Propellant transfer requires that the liquid be completely settled with virtually no bubbles. Outflow of a liquid near the tank outlet can result in the premature ingestion of gas while a significant amount of liquid is still in the tank under microgravity environment. This phenomenon is termed "suction dip." Slosh wave motion must be minimal because the combination of suction dip and sloshing could cause gas pull-through to occur more readily in microgravity than if the surface were essentially quiescent.

During the prepressurization of a cryogenic propellant in microgravity, significant heat and mass transfer will occur if the liquid interface is disturbed. Interface disturbances may result from 1) impingement of the gas on the liquid surface at a mass flow rate sufficient to cause Kelvin-Helmholtz instability, 2) globule formation from breaking waves caused by wave motion over baffles or internal hardware, 3) globule and surface froth formation resulting from movement of bubbles through the liquid to the surface, and 4) surface froth formation because of gas impingement.

Bubble and globule formation as a result of liquid impact with the aft end of the tank could lead to propellant loss for the spacecraft during venting. Globules could be entrained in the vented ullage gas or bubbles rising through the liquid and expansion because of the decreasing tank pressure could cause a spray of globules to be vented. Liquid-level rise, vent-liquid loss, fluid freezing, and vehicle dynamics are all affected by the microgravity levels.

Recently, Leslie[2] performed a series of measurements on rotating equilibrium, free-surface shapes in the microgravity environment of a free-falling aircraft (KC-135). The apparatus consisted of a Plexiglass cylinder with different depths. The cylinder was partially filled with ethanol, chosen because 1) its surface tension is relatively high (2.28×10^{-2} N/m) with air at 1 atm and 20°C; 2) the value of surface tension is not very sensitive to low levels of contamination; 3) its contact line with the container does not stick; and 4) its contact angle is close to zero. Because the evaporation rate of ethanol is very small at room temperature, volume conservation can be assumed during the course of an experiment. The cylinder was fastened to a turntable that rotated about the cylinder's axis. After the cylinder was filled with ethanol, a prescribed amount was removed to establish the bubble volume.

Leslie[2] was able to measure and to compute numerically the bubble shapes at various ratios of centrifugal force to surface tension force in 2-, 4-, and 6.3-cm-deep cylinders in the microgravity environment. The results showed excellent agreement between model computation and measurements. Hung and Leslie[3] extended Leslie's work[2] to rotating free surfaces influenced by gravity with higher rotating speeds when the bubble intersects with both the top and bottom walls of the cylinder. Hung et al.[4,5] further extended the work to include rotating free surfaces influenced by different levels of gravity forces with different rotating speeds, which resulted from bubbles intersecting with and/or without intersecting the top, bottom, and side walls of the cylinder.

An analysis of time-dependent dynamical behavior of surface tension on partially filled rotating fluids in both low-gravity and microgravity environments was carried out by numerically solving the Navier-Stokes equations subjected to the initial and the boundary conditions.[4,6] At the interface between the liquid and the gaseous fluids, both the kinematic surface boundary condition and the interface stress conditions for components tangential and normal to the interface were applied. The initial condition for the bubble profiles was adopted from steady-state formulations developed by Hung and Leslie,[3] and Hung et al.[6] for rotating cylinder tank; and by Hung et al.[5,7] for the Gravity Probe-B Spacecraft.[8] Some of the steady-state formulations of bubble shapes, in particular for bubbles intersecting the top wall of the cylinder, were compared with the experiment carried out by Leslie[2] in a free-falling aircraft (KC-135). Comparisons of time-dependent results between numerical computations and experiments were unavailable. This was because the calibration of the recordings of time-dependent gravity variations in a KC-135 aircraft during the short periods of microgravity is very difficult. There was also an unavailability of accelerometer data for measuring the actual levels of microgravity during the experiment.

In this study, time-dependent computations have been carried out to investigate the dynamical behavior of fluid reorientation or resettling of propellant prior to main engine firing for spacecraft restart. The computation extends to the study of the characteristics of fluid resettlement caused by the reversal of gravity fields with and without gravity jitter. Positioning of liquid propellant over the tank outlet can be carried out by using small auxiliary thrusters that provide a thrust parallel to the tank's major axis in the direction of flight. Gravity jitters imposed on the liquid propellant can be induced by pulsating of small auxiliary thrusters.

II. Mathematical Formulation

Consider a closed-circular cylinder of radius a with length L, which is partially filled with a Newtonian fluid of constant density ρ and kinematic viscosity ν. The cylinder rotates about its axis of symmetry with angular velocity $\omega(t)$ which is a function of time t.

Cylindrical coordinates (r,θ,z) will be used, with the corresponding velocity components (u,v,w). The gravitational acceleration g is along the z axis. For the case of axial symmetry, the θ dependency vanishes. The governing equations are shown as follows:

Continuity Equation:

$$\frac{1}{r}\frac{\partial}{\partial r}(ru) + \frac{\partial w}{\partial z} = 0 \tag{1}$$

Momentum Equations:

$$\frac{\mathrm{D}u}{\mathrm{D}t} - \frac{v^2}{r} = -\frac{1}{\rho}\frac{\partial P}{\partial r} + \nu\left(\nabla^2 u - \frac{u}{r^2}\right) \tag{2}$$

$$\frac{\mathrm{D}v}{\mathrm{D}t} + \frac{uv}{r} = \nu\left(\nabla^2 v - \frac{v}{r^2}\right) \tag{3}$$

$$\frac{\mathrm{D}w}{\mathrm{D}t} = \frac{1}{\rho}\frac{\partial P}{\partial z} - g + \nu\nabla^2 w \tag{4}$$

where

$$\frac{\mathrm{D}}{\mathrm{D}t} = \frac{\partial}{\partial t} + u\frac{\partial}{\partial r} + w\frac{\partial}{\partial z} \tag{5}$$

$$\nabla^2 = \frac{1}{r}\frac{\partial}{\partial r}\left(r\frac{\partial}{\partial r}\right) + \frac{\partial^2}{\partial z^2} \tag{6}$$

Let the profile of the interface between gaseous and liquid fluids be given by

$$\eta(t,r,z) = 0 \tag{7a}$$

or

$$r = \eta(t,z) \tag{7b}$$

The initial condition of the profile of interface between the gaseous and liquid fluids at $t = t_0$ is assigned explicitly, and is given by

$$\eta(t=t_0,r,z) = 0 \tag{8a}$$

or

$$r = \eta_0(z) = \eta(t_0,z) \tag{8b}$$

A set of boundary conditions has to be supplied for solving the equations. The initial interface profiles used in this study were obtained explicitly from the steady-state computations made by Hung and Leslie[3] and Hung et al.,[6] which were checked by the experiments carried out by Leslie.[2] These boundary conditions are as follows:

1) At the container wall, no-penetration and no-slip conditions assure that both the tangential and the normal compo-

nents of the velocity along the solid walls will vanish. In the numerical calculation of bubble profiles for ethanol and air, a constant contact angle is present when the free surface of liquid ethanol intersects the container wall.

2) Along the interface between the liquid and gaseous fluids, the following two conditions apply:

a) Kinematic surface boundary condition: The liquid (or gaseous) surface moves with the liquid (or gas) which implies

$$\frac{D\eta}{Dt} = 0 \tag{9a}$$

or

$$\frac{\partial \eta}{\partial t} + u\frac{\partial \eta}{\partial r} + w\frac{\partial \eta}{\partial z} = 0 \tag{9b}$$

$$\text{on } \eta = \eta\ (t = t_i, r, z)$$

b) Interface stress condition: At the interface, the stresses must be continuous. These can be decomposed into the components normal and tangential to the interface. For the component tangential to the interface between liquid and gaseous fluids,

$$\left[\tau \cdot n - (n \cdot \tau \cdot n)\right]_{\text{liquid}} = \left[\tau \cdot n - (n \cdot \tau \cdot n)\right]_{\text{gas}} \tag{10}$$

must hold. Here, the viscous stress tensor is

$$\tau_{ij} = \mu\left(\frac{\partial u_i}{\partial x_j} + \frac{\partial u_j}{\partial x_i} - \frac{2}{3}\frac{\partial u_k}{\partial x_k}\delta_{ij}\right) + \zeta\frac{\partial u_k}{\partial x_k}\delta_{ij}$$

For the component normal to the interface between the liquid and gaseous fluids, the expression becomes Laplace's formula, which is the following:

$$P_G - P_L - (n \cdot \tau \cdot n)_{\text{gas}} + (n \cdot \tau \cdot n)_{\text{liquid}} = -\frac{\sigma}{r}\frac{d}{dr}\left[\frac{r\phi}{(1+\phi^2)^{1/2}}\right] \tag{11}$$

The tangent of the interface is defined by

$$\phi = \frac{dz}{dr}$$

$$\text{on } \eta_i = \eta(t_i, r, z) \tag{12}$$

III. Numerical Simulation of Fluid Behavior Under Microgravity Environments

The present study examined time-dependent fluid behavior, in particular the dynamics of the bubble configurations, under microgravity environments. The initial bubble profiles are determined from computations based on algorithms developed in our earlier studies.[3-7] In other words, the initial bubble profiles computed from the steady-state formulation, in conjunction with the following parameters (such as liquid density ρ_L and its kinematic viscosity ν_L; gas density ρ_G and its kinematic viscosity ν_G; surface tension coefficient σ, angular velocity ω, and gravity environment g, etc.) are used as the initial input for the time-dependent computation. Thus, the initial condition at the interface profile between gaseous and liquid fluids at $t = t_0$ can be assigned explicitly with Eq. (8).

A staggered grid for the velocity components is used in this computer program. The method was first developed by Harlow and Welch[9] for their MAC (Marker and Cell) method of studying fluid flows along free surface. Figure 1a shows a three-dimensional schematic expression for the distribution of grid points in cylindrical coordinates. Figure 1b shows staggered locations in the r-z plane in which "→" denotes staggered locations for the radial component of the velocity u; "↑" denotes the axial component of the velocity w; and "O" denotes the other variables such as pressure.

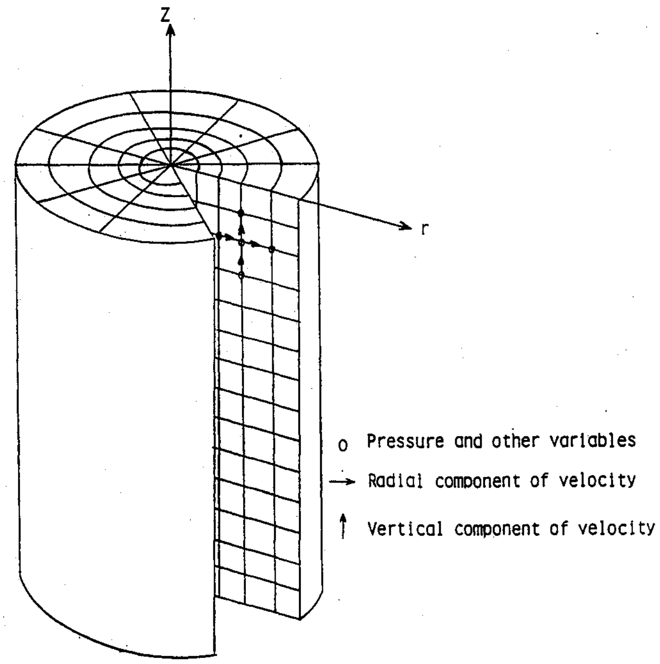

Fig. 1a Three-dimensional schematic expression of the distribution of grid points in cylindrical coordinates.

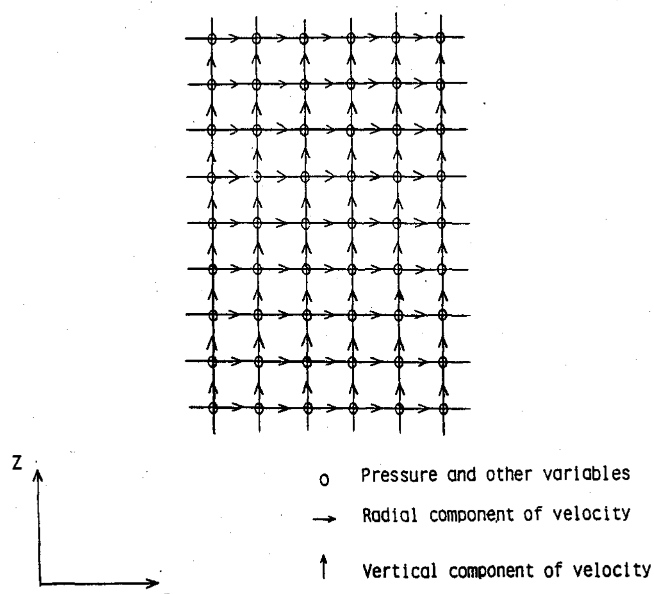

Fig. 1b Staggered location in the r-z plane in which "→" denotes staggered location for the radial component of velocity; "↑" denotes the axial component of velocity; and "O" denotes other variables, such as pressure.

The finite-difference method employed in this numerical study was the "Hybrid Scheme" developed by Spalding.[10] The formulation for this method is valid for any arbitrary interface location between the grid points and is not limited to middle point interfaces.[10] An algorithm for the semi-implicit method[11,12] was used as the procedure for modeling the flowfield. The time step is determined automatically based on the size of the grid points and the angular velocity of the rotating fluids.

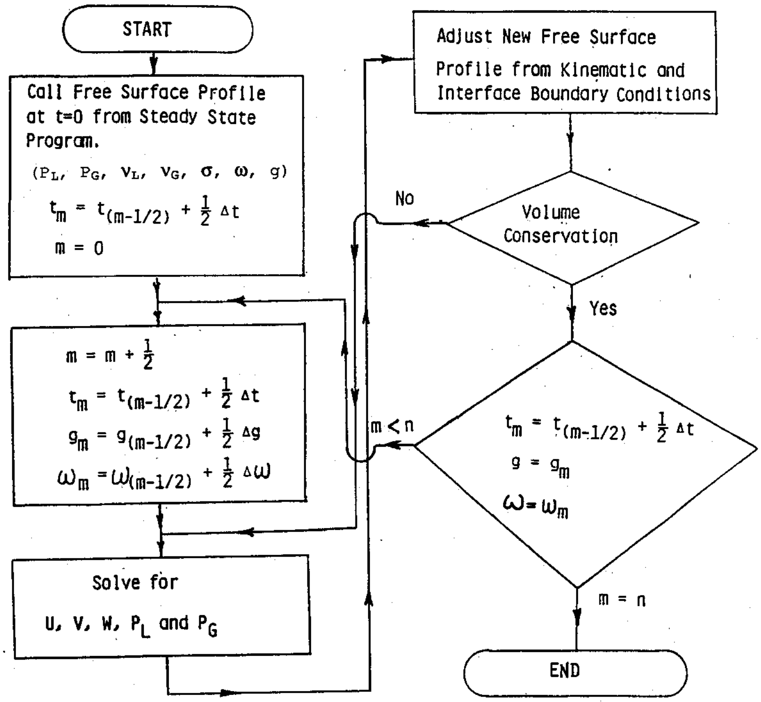

Fig. 2 Flowchart for the procedures of computation for numerically determining time-dependent evolution of the bubble shapes.

A computer algorithm was developed to integrate Eqs. (1–4) numerically, subjected to the following conditions: 1) initial condition, Eq. (8); 2) boundary conditions, which include no-penetration and no-slip conditions at the container wall; 3) a kinematic surface boundary condition, shown in Eq. (9); and 4) interface stress conditions, shown in Eqs. (10–12). Figure 2 illustrates the flowcharts for the computational procedures for numerically solving these equations.

For the purpose of facilitating easy comparison between computational results and experimental measurements [partially liquid-filled rotating cylinder with free surfaces in the low and microgravity environments of a free-falling aircraft (KC-135), carried out by Leslie[2]], a container radius of 2 cm and a height of 5 cm is assumed. The numerical computations have been performed by CRAY X-MP supercomputers at both NASA Marshall Space Flight Center and the Alabama Super Computer Center. In this study, the gravitational field is taken to be parallel to the major axis of the cylindrical coordinate system, and, unless otherwise stated, it is always pointing in the downward direction.

Behavior of the liquid propellant becomes uncertain when the gravity environment is reduced on the order of $10^{-6}g_0$ level ($g_0 = 9.81$ m/s^2). The requirement to settle or to position liquid fuel over the outlet end of the spacecraft propellant tank prior to main engine restart poses a microgravity fluid behavior problem. Retromaneuvers of spacecraft, such as the orbital maneuvering vehicle (OMV) and space transfer vehicle (STV)[13] during flight from high Earth orbit to low Earth orbit, require settling or reorientation of the propellant prior to main engine firing. Cryogenic liquid propellant is positioned over the tank outlet by using small auxiliary thrusters (or idle-mode thrusters from the main engine), which provide a thrust parallel to the tank's major axis in the direction of flight. During the reorientation process, the liquid flows in an annular sheet along the tank wall, with the gas or ullage bubble "rising" centrally into the liquid. This motion would also clear the tank vent of liquid so that venting of vapor is possible.

An efficient propellant-settling technique should minimize propellant usage and weight penalties. This can be accomplished by providing optimal acceleration to the spacecraft such that the propellant is reoriented over the tank outlet without any vapor entrainment, any excessive geysering, or any other undesirable fluid motion.

In this study, a 2 cm radius by 9 cm high tank partially filled with ethanol and with a volume of air equal to 40% of the tank is considered. The air bubble is originally positioned at the bottom of the tank. In other words, to provide conservative settling conditions, the liquid is assumed to be initially oriented at the top of the tank. If the spacecraft has been coasting for a long time, aligned with its direction of motion, the most significant force, drag, would be axial. At time $t = 0$, acceleration with a net value of $0.03g_0$ is applied toward the downward direction of the tank's major axis. The time evolution of the fluid reorientation is calculated.

A. Fluid Reorientation of Nonrotating Container Without Gravity Jitter

The rotating speed is assumed to be $\omega = 0$, which is true for the OMV and STV,[13] in this case. Figures 3a–3f show the sequence of time evolution of fluid reorientation for nonrotating liquid tank without the effect of gravity jitter. The following conclusions can be drawn: 1) The liquid starts to flow in an annular sheet along the solid wall of the tank and gradually pushes the bubble toward the central portion of the lower dome of the tank as the net acceleration, reversing the direction of gravity field, is applied toward the downward direction of the tank's major axis (see Figs. 3b and 3c), by using small auxiliary thrusters. 2) As the downward fluid annular sheet along the tank wall reaches the central bottom dome side of the tank, a geysering flow is observed (see Figs. 3d and 3e). 3) The bubble is thus pushed upward centrally into the liquid and the geysering disappears (see Fig. 3f).

Table 1 shows the characteristics of fluid settlement for case A. It shows that the time required for the resettling liquid to reach the middle point of the lower dome of the propellant tank is 0.694 s; the time for the initiation of the geyser when the liquid reaches the tip of the bottom of the lower dome of the tank is 0.788 s; and the time for the termination of geyser after the liquid pushes up the bubble and leaves the bottom solid wall of the tank is 1.04 s. The time period between termination and initiation of geyser is 0.252 s for this case.

B. Fluid Reorientation of Rotating Container Without Gravity Jitter

Some spacecraft, such as Gravity Probe-B,[8] will be rotating with respect to the major axis of the propellant tank in the

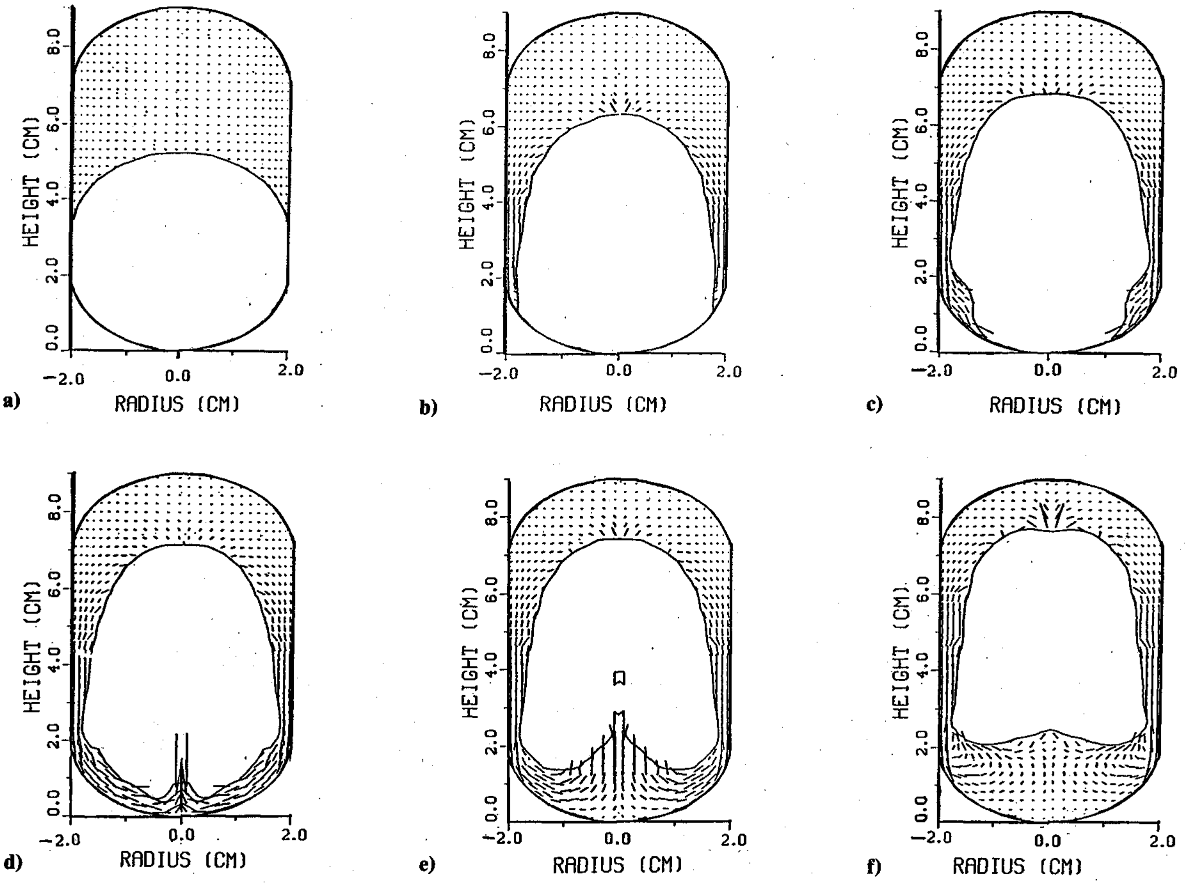

Fig. 3 Nonrotating fluid reorientation without gravity jitter for liquid ethanol and air bubble for a net acceleration of $0.03g_0$: a) at $t = 0.0532$ s; b) at $t = 0.480$ s; c) at $t = 0.694$ s; d) at $t = 0.788$ s; e) at $t = 0.880$ s; and f) at $t = 1.04$ s.

orbit. A time-series evolution of the fluid reorientation for a rotating liquid tank ($\omega = 10$ rpm) without the effect of gravity jitter was computed. These profiles are illustrated in Figs. 4a–4f. All of the parameters used are similar to that of Fig. 3 except for the rotating speed of the liquid tank. The following conclusions can be made: 1) All of the statements applicable to Fig. 3 are true including the dynamical behavior of the liquid flow in an annular sheet along the tank wall (see Figs. 4b and 4c); a geysering flow was also detected when fluid reached the central, bottom side of the lower dome of the tank (see Fig. 4d) and a bubble rose centrally into the fluid (see Fig. 4e). 2) The effect of centrifugal force pushes the liquid away from the central axis of rotation toward the vertical sidewalls of the cylindrical tank. Dynamics of this annular sheet of fluid, which was pushed radially by the mild centrifugal force (rotation speed less than 30 rpm), along the solid wall are governed by the balance of: adhesive force between liquid and solid wall, surface tension force of the liquid, downward gravity force induced by the auxiliary thruster, and the centrifugal force. In other words, the motions are as follows: a) the liquid was pushed radially outward along the solid wall in the form of an annular sheet; b) the fluid flows downward along the solid wall to the bottom of the tank; and c) the bubble was gradually pushed up centrally by the downward flowing liquid. The acceleration of liquid flowing downward along the side wall is viewed as being caused by the effects of centrifugal force that pushes the liquid radially outward along the sidewall of the tank.

Table 1 also shows the characteristics of fluid settlement for case B. It shows that the time required for the resettling liquid to reach the middle point of the lower dome of the propellant tank is 0.64 s, which is shorter than that of case A; the time for the initiation of geyser when the liquid reaches the tip of the bottom of the lower dome of the tank is 0.781 s, which is again earlier than that of case A; and the time for the termination of geyser after the liquid pushes up the bubble and leaves the bottom solid wall of the tank is 0.941 s, which is also earlier than that of the case A. The time period between termination and initiation of geyser is 0.16 s, which is again shorter than that of case A. As we indicated earlier, an efficient propellant-settling technique should minimize propellant usage made by the operation of small auxiliary thrusters. It should also reorient the propellant over the tank outlet without any vapor entrainment and any excessive geysering. In this respect, the propellant-settling technique for spacecraft with a rotating fluid tank is superior to that of a spacecraft without a rotating fluid tank.

Table 1 Characteristics of fluid resettlement[a]

Case	A	B	C	D
Rotating speed, rpm	0	10	0	0
Frequency of gravity jitters, Hz	0	0	2.0	1.0
Resettling fluid reaching the middle of the lower dome, s	0.694	0.64	0.628	0.56
Initiation of geyser, s	0.788	0.781	0.645	0.635
Termination of geyser, s	1.04	0.941	0.879	0.875
Time period of geyser, s	0.252	0.16	0.134	0.24

[a] Fluids: Ethanol and air. Background gravity: $g_b = 0.03g_0$.

C. Fluid Reorientation of Nonrotating Container with Higher Frequency of Gravity Jitters

Fluid reorientation subjected to the effects of the vibrations of the gravity environment has also been studied. Vibration of the gravity environment (gravity jitters) is governed by the following formula:

$$g = g_b\left[1 + \tfrac{1}{2}\sin(2\pi f_0 t)\right] \tag{13}$$

where g_b denotes the background gravity environment, and f_0 (Hz) stands for the vibration frequency (frequency of gravity jitters).

Gravity jitters imposed on the liquid propellant is nothing but the use of imposed oscillatory motions by applying the pulse type of turning on and off of small auxiliary thrusters. This pulse method of operating small auxiliary thrusters can introduce oscillatory acceleration (gravitation) to the major axis of the tank in the direction of flight for the positioning of liquid propellant over the tank outlet prior to main engine firing.

In this case, a nonrotating fluid tank with a higher frequency of gravity jitters of 2 Hz is considered in the computation. Figures 5a–5f show that the sequence of time evolution of fluid reorientation is similar to that described in case A.

Table 1 also shows the characteristics of fluid settlement for case C. It shows that the time required for the resettling liquid to reach the middle point of the lower dome of the propellant tank is 0.628 s, which is shorter than that of cases A and B; the time for the initiation of geyser when the liquid reaches the tip of the bottom of the lower dome of tank is 0.645 s, which is again earlier than that of cases A and B; and the time for the termination of geyser after the liquid pushes up the bubble and leaves the bottom solid wall of the tank is 0.879 s, which is also earlier than that of cases A and B. The time period between termination and initiation of geyser is 0.134 s, which is shorter than that of cases A and B for this case. In view of the criteria to achieve an efficient propellant-settling technique, a gravity-jitter frequency with 2 Hz imposed on the fluid reorientation through the pulse type of turning on and off of the auxiliary thrusters can improve the performance of fluid resettlement. This occurs because case C takes a shorter time to accomplish the task of fluid settling and a shorter period of time during the initiation and termination of geysering than that without applying gravity jitters.

D. Fluid Reorientation of Nonrotating Container with Lower Frequency of Gravity Jitters

A nonrotating fluid tank with lower-frequency gravity jitters of 1 Hz is considered in the computation of case D. Figures 6a–6f show the sequence of time evolution of fluid reorientation for the case D. Again the basic features for the dynamic behavior of the fluid reorientation are similar to that described in case A.

Table 1 shows the characteristics of fluid settlement for case D. It shows that the time required for the settling liquid to reach the middle point of the lower dome of the propellant tank is 0.56 s, which is shorter than that of cases A, B, and C; the time for the initiation of geyser when the liquid reaches the tip of the bottom of the lower dome of tank is 0.635 s, which is again earlier than that of cases A, B, and C; and the time for the termination of geyser after the liquid pushes up the bubble and leaves the bottom solid wall of the tank is 0.875 s, which is also earlier than that of cases A, B, and C. However, the time period between the termination and initiation of the geyser is 0.24 s, which is longer than that of cases B and C for this case. In view of the criteria necessary for an efficient propellant-settling technique, a lower gravity-jitter frequency with 1 Hz imposed on the fluid reorientation is not necessarily

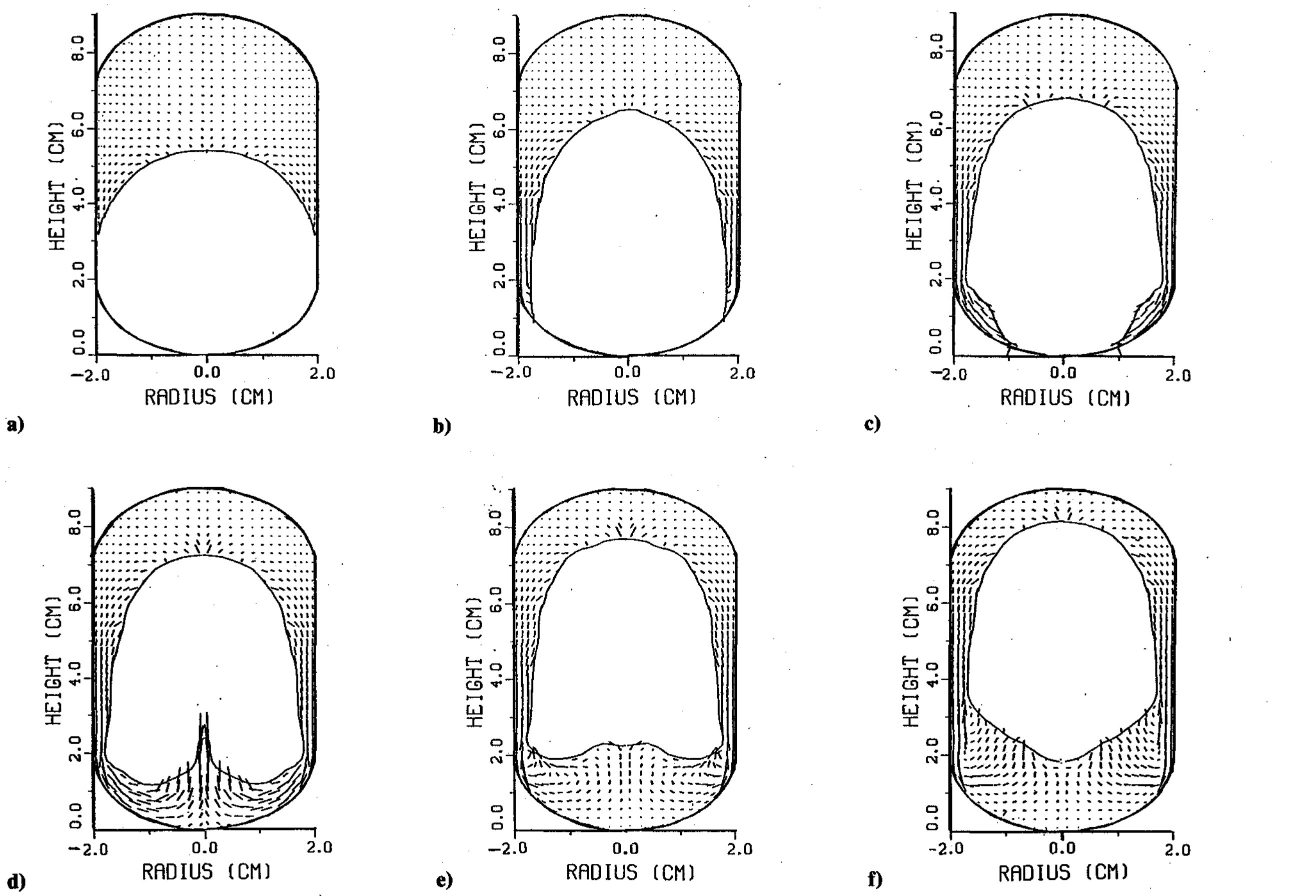

Fig. 4 Rotating fluid reorientation ($\omega = 10$ rpm) without gravity jitter for liquid ethanol and air bubble for a net acceleration of $0.03g_0$: a) at $t = 0.16$ s; b) at $t = 0.48$ s; c) at $t = 0.64$ s; d) at $t = 0.781$ s; e) at $t = 0.941$ s; and f) at $t = 1.10$ s.

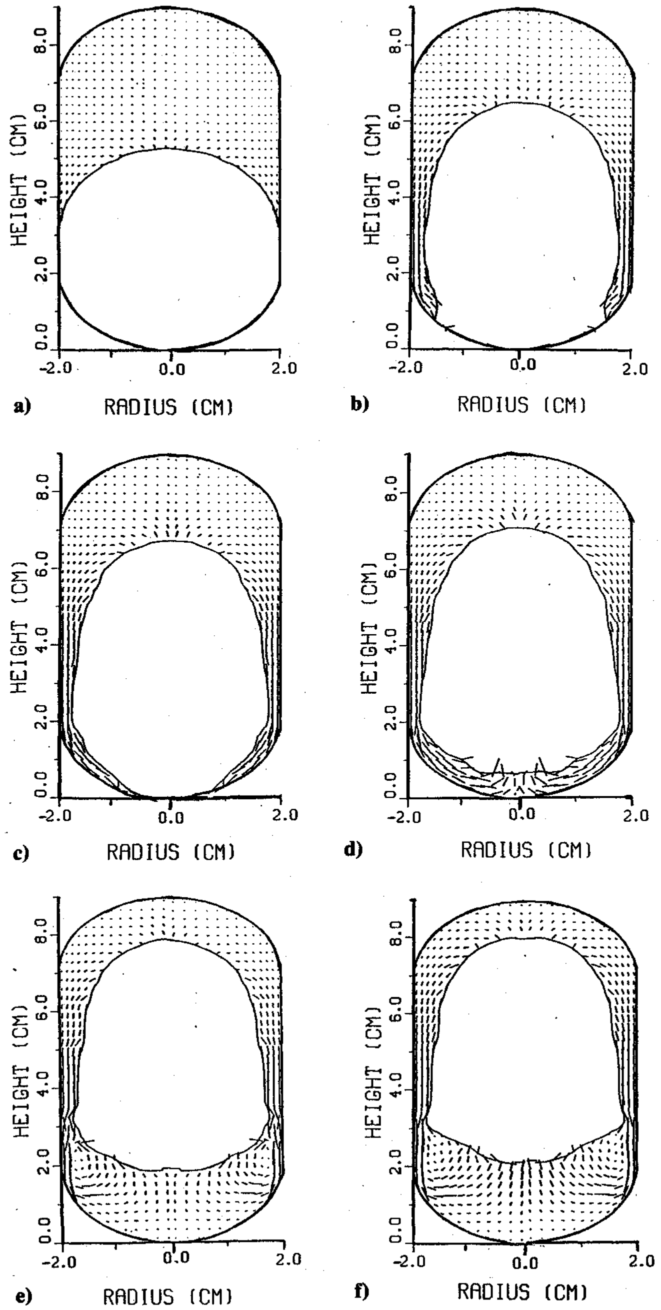

Fig. 5 Nonrotating fluid reorientation with higher gravity-jitter frequency ($f = 2$ Hz) for a net acceleration of $0.03 g_0$: a) at $t = 0.0799$ s; b) at $t = 0.560$ s; c) at $t = 0.639$ s; d) at $t = 0.719$ s; e) at $t = 1.04$ s; and f) at $t = 1.12$ s.

better than that of a rotating container and a nonrotating container with a higher gravity-jitter frequency. This occurs because although case D takes a shorter time to accomplish the task of fluid settling, it takes a longer period of time during the initiation and termination of geysering than that of cases B and C. More extensive studies would need to be done to select properly the frequencies of gravity jitters (the imposed oscillatory motions induced by the auxiliary thruster) before one can determine the best parameters to be used for carrying out fluid reorientation.

Recently, the time evolution of slosh waves excited by the gravity jitters and centrifugal forces were studied in detail.[14,15] The results show that there is a group of wave trains, both in longitudinal and transverse modes, with various frequencies and wavelengths of slosh waves. These are generated by the restoring force field of gravity jitters and centrifugal forces assumed in this study.[14,15] The longest wave periods of the slosh waves, either longitudinal or transverse modes, are responsible for the production of wave modes with the highest ratio of maximum wave amplitude to wavelength. Between longitudinal and transverse slosh waves, the longest wave period transverse modes produce a greater ratio of maximum wave amplitude to wavelength wave mode than that of the longitudinal slosh waves.[14,15] In any case, the effect of gravity jitters on the purpose of resolving an efficient propellant-settling technique must be studied extensively before a definitive conclusion on this subject can be reached.

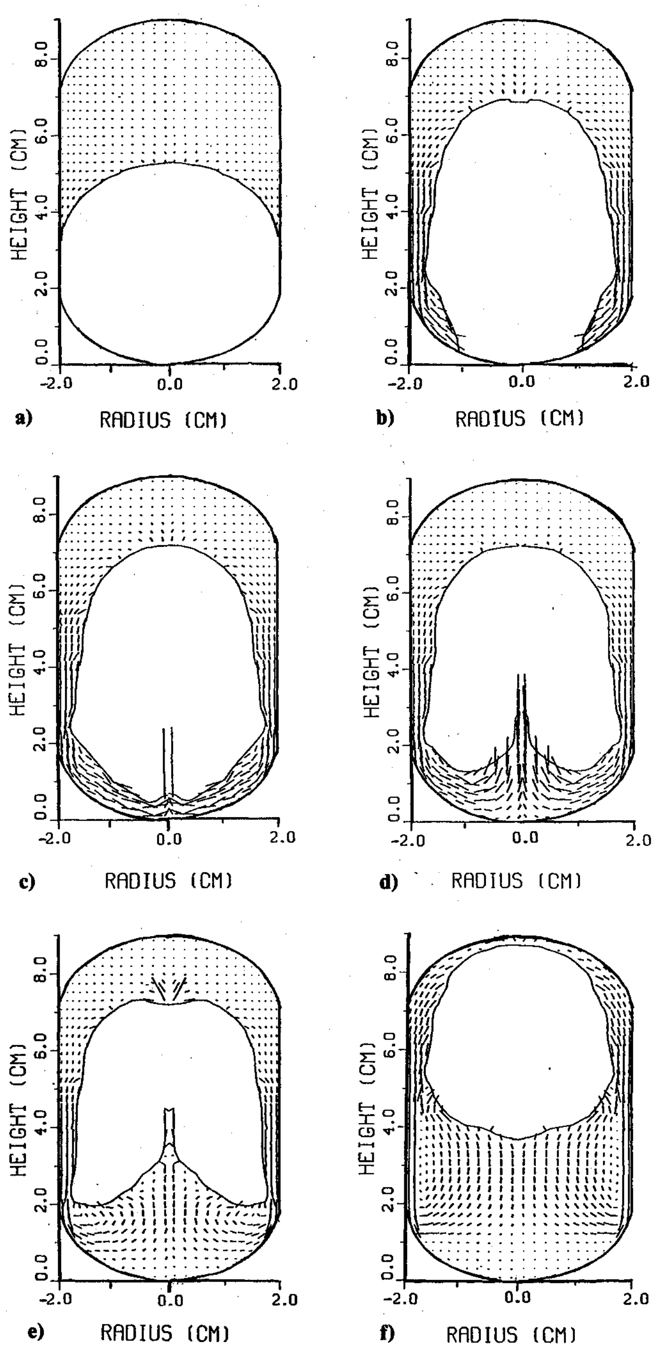

Fig. 6 Nonrotating fluid reorientation with lower gravity-jitter frequency ($f = 1.0$ Hz) for a net acceleration of $0.03 g_0$: a) at $t = 0.0799$ s; b) at $t = 0.560$ s; c) at $t = 0.635$ s; d) at $t = 0.697$ s; e) at $t = 0.857$ s; and f) at $t = 1.50$ s.

IV. Discussion and Conclusion

The dynamical behavior of fluids, in particular, the effect of surface tension on partially filled rotating fluids in a microgravity environment has been carried out by numerically solving the Navier-Stokes equations subject to initial and boundary conditions. At the interface between the liquid and gaseous fluids, both the kinematic surface boundary condition, and the interface stress conditions, have been applied. The initial conditions of the bubble profiles were adopted from steady-state solutions developed by Hung and Leslie,[3] and Hung et al.[4-7]

Cryogenic liquid propellant is required to position the fluid over the tank outlet by using small auxiliary thrusters that provide a thrust parallel to the tank's major axis in the direction of flight. To provide conservative settling conditions, the liquid was assumed to be initially oriented at the top of the tank. If the spacecraft has been coasting for a long time, aligned with the direction of motion, the most significant force, drag, would be axial. Axisymmetric representation of the tank, with a cylindrical coordinate system, was assumed. The settling acceleration was assumed to be parallel to the axial direction, and the liquid was initially oriented symmetrically at the top of the tank.

The results of the study of fluid reorientation have to be evaluated in terms of how well they can be managed efficiently. An efficient propellant-settling technique should minimize propellant usage and weight penalties through the operation of small thrusters (or idle-mode thrusters from the main engine). This can be accomplished by providing optimal acceleration to the spacecraft such that the propellant is reoriented over the tank outlet without any vapor entrainment, any excessive geysering, or any other undesirable fluid motion.

Four cases of fluid reorientation have been studied. These include fluid settlement in rotating and nonrotating tanks, and with and without higher- and lower-frequency gravity jitters imposed on the fluid reorientation. Results show that the resettlement of fluid can be accomplished more efficiently for fluid in a rotating tank than in a nonrotating tank based on the amount of time needed to carry out resettlement and the period of time between the initiation and termination of geysering. It also shows that with a proper choice of the frequency of gravity jitters (the imposed oscillatory motions induced by the auxiliary thruster) imposed on the fluid reorientation the propellant-settling technique can be accomplished more efficiently than that of fluid reorientation without gravity jitters. Recently, characteristics of slosh waves excited by the gravity jitters have been studied.[14,15]

Results show that lower-frequency gravity jitters (imposed oscillatory motions by using pulse-type operation of small auxiliary thruster) excited slosh waves with a higher ratio of maximum amplitude to wavelength than that of slosh waves excited by higher-frequency gravity jitters.[14,15] The present study shows that the lower gravity-jitter frequency imposed on the fluid reorientation is not necessarily better than that of a rotating container or a nonrotating container with a higher gravity-jitter frequency. This is because although lower gravity-jitter frequency imposed on the fluid reorientation takes shorter time to accomplish the task of fluid settling, it takes a longer time period for geysering (a time period between initiation and termination of geysering) than the cases of rotating tank and higher gravity-jitter frequency without rotation. More extensive studies will be necessary to select properly the frequencies of the gravity jitter and the optimal acceleration before the best parameters to be used in carrying out an efficient fluid-settling technique can be determined.

Any fluid capable of motion relative to the spacecraft will be subject to an acceleration relative to the mass center of the spacecraft that arises from the gravity gradient of the Earth.[16,17] In addition to the Earth's gravitational force, the interaction between the particle mass of fluids and the spacecraft mass caused by gravity-gradient accelerations[16] have also been taken into consideration in this microgravity fluid-management study.

To conclude, we have demonstrated that the computer algorithm presented can be used to simulate fluid behavior in a microgravity environment and provide proper design techniques for handling and managing the cryogenic liquid propellants to be used in spacecraft propulsion.

Acknowledgment

The authors appreciate the support received from NASA Headquarters through NASA Grant NAGW-812, and NASA Marshall Space Flight Center through NASA Contract NAS8-36955/Delivery Order 69.

References

[1]Kamotani, Y., Prasad, A., and Ostrach, S., "Thermal Convention in an Enclosure Due to Vibrations Aboard a Spacecraft," *AIAA Journal*, Vol. 19, 1981, pp. 511–516.

[2]Leslie, F. W., "Measurements of Rotating Bubble Shapes in a Low-Gravity Environment," *Journal of Fluid Mechanics*, Vol. 161, 1985, pp. 269–279.

[3]Hung, R. J., and Leslie, F. W., "Bubble Shape in a Liquid-Filled Rotating Container Under Low Gravity," *Journal of Spacecraft and Rockets*, Vol. 25, No. 1, 1988, pp. 70–74.

[4]Hung, R. J., Tsao, Y. D., Hong, B. B., and Leslie, F. W., "Time-Dependent Dynamical Behavior of Surface Tension on Rotating Fluids Under Microgravity Environment," *Advances in Space Research*, Vol. 8, No. 12, 1988, pp. 205–213.

[5]Hung, R. J., Tsao, Y. D., Hong, B. B., and Leslie, F. W., "Bubble Behaviors in a Slowly Rotating Helium Dewar in Gravity Probe-B Spacecraft Experiment," *Journal of Spacecraft and Rockets*, Vol. 26, 1989, pp. 167–172.

[6]Hung, R. J., Tsao, Y. D., Hong, B. B., and Leslie, F. W., "Dynamical Behavior of Surface Tension on Rotating Fluids in Low and Microgravity Environments," *International Journal for Microgravity Research and Applications*, Vol. 11, 1989, pp. 81–95.

[7]Hung, R. J., Tsao, Y. D., Hong, B. B., and Leslie, F. W., "Axisymmetric Bubble Profiles in a Slowly Rotating Helium Dewar Under Low and Microgravity Environments," *Acta Astronautica*, Vol. 19, 1989, pp. 411–426.

[8]"Stanford Relativity Gyroscope Experiment (NASA Gravity Probe-B)," *Proceedings of Society of Photo-Optical Instrumentation Engineers*, Vol. 619, Society of Photo-Optical Instrumentation Engineers, Bellingham, WA, 1986, pp. 1–165.

[9]Harlow, F. H., and Welch, F. E., "Numerical Calculation of Time-Dependent Viscous Incompressible Flow of Fluid with Free Surface," *Physics of Fluids*, Vol. 8, 1965, pp. 2182–2189.

[10]Spalding, D. B., "A Novel Finite-Difference Formulation for Differential Expressions Involving Both First and Second Derivatives," *International Journal of Numerical Methods in Engineering*, Vol. 4, 1972, pp. 551–559.

[11]Patanker, S. V., *Numerical Heat Transfer and Fluid Flow,* Hemisphere-McGraw-Hill, New York, 1980, p. 197.

[12]Patanker, S. V., and Spalding, S. D., "A Calculation Procedure for Heat, Mass, and Momentum Transfer in Three-Dimensional Parabolic Flows," *International Journal of Heat Mass Transfer*, Vol. 15, 1972, pp. 1787–1805.

[13]NASA Office of Aeronautics and Space Technology, *Technology for Future NASA Missions: Civil Space Technology Initiative and Pathfinder*, NASA CP-3016, 1988, p. 568.

[14]Hung, R. J., Lee, C. C., and Leslie, F. W., "Effect of *G*-Jitters on the Stability of Rotating Bubble Under Microgravity Environment," *Acta Astronautica*, Vol. 21, 1990, pp. 309–321.

[15]Hung, R. J., Tsao, Y. D., and Leslie, F. W., "Response of Gravity-Level Fluctuations on the Gravity Probe-B Spacecraft Propellant System," *Journal of Propulsion and Power* (to be published).

[16]Misner, C. W., Thorne, K. S., and Wheeler, J. A., *Gravitation*, Freeman and Co., San Francisco, 1973, pp. 1279.

[17]Forward, R. L. "Flattening Space-Time Near the Earth," *Physical Review D*, Vol. 26, 1982, pp. 735–744.

Henry B. Garrett
Associate Editor